Biophysical Journal
Biophysical Letter

Biophysical Society

Deuterium-Enhanced Raman Spectroscopy for Histidine pK_a Determination in a pH-Responsive Hydrogel

Gabriel A. Braun,[1,2,*] Brett H. Pogostin,[1] Milda Pucetaite,[3] Casey H. Londergan,[1] and Karin S. Åkerfeldt[1]
[1]Department of Chemistry, Haverford College, Haverford, Pennsylvania; [2]Centre for Molecular Protein Science, Department of Biochemistry and Structural Biology, Lund University, Lund, Sweden and [3]Centre for Environmental and Climate Research, Lund University, Lund, Sweden

ABSTRACT We report here a method for the determination of the pK_a of histidine in complex or heterogeneous systems amenable to neither solid-state nor solution NMR spectroscopy. Careful synthesis of a fluorenylmethyloxycarbonyl- and trityl-protected, C2-deuterated histidine produces a vibrational-probe-equipped amino acid that can readily be incorporated into any peptide accessible by standard solid-phase methods. The frequency of the unique, Raman-active stretching vibration of this C2-D probe is a clear reporter of the protonation state of histidine. We investigate here a pH-sensitive peptide that self-assembles to form a hydrogel at neutral pH. The pK_a of the lone histidine residue in the peptide, which is likely responsible for this pH-dependent behavior, cannot be investigated by NMR spectroscopy because of the supramolecular, soft nature of the gel. However, after synthesizing a C2-deuterated-histidine-containing peptide, we were able to follow the protonation state of histidine throughout a pH titration using Raman difference spectroscopy, thereby precisely determining the pK_a of interest.

SIGNIFICANCE We report a broadly applicable Raman-spectroscopy-based method for histidine pK_a determination in systems that are challenging to study by traditional means such as NMR spectroscopy. Using standard solid-phase peptide synthesis, we incorporated a C2-deuterated histidine into a hydrogel-forming peptide, employing a modified fluorenylmethyloxycarbonyl-deprotection protocol. This resulted in a protonation-sensitive vibrational probe that allowed us to precisely determine the pK_a of the histidine residue as the peptide underwent self-assembly to form a hydrogel.

Accurate determination of the pK_a of histidine is crucial in understanding the activity of many pH-responsive systems because the protonation state of histidine has important functional implications for the behavior of both biological (1,2) and synthetic (3,4) proteins and peptides. The protonation state of histidine is known to play an important role in certain amyloid-forming systems; for example, amyloid formation by human islet amyloid polypeptide is highly pH dependent, owing to a key histidine residue (5). Knowledge of the pK_a of histidine in aggregate states is also important for the design of pH-responsive biomaterials such as hydrogels (6). The pK_a of histidine residues is typically determined using solution NMR spectroscopy (7,8), although magic-angle spinning solid-state NMR can also be used for this purpose (9,10). However, solution NMR is poorly suited to study large supramolecular assemblies because of line broadening caused by the slow tumbling of such species (11), whereas magic-angle spinning NMR is limited to immobilized samples and can be particularly challenging to use with soft materials such as hydrogels (12,13).

Raman spectroscopy provides an alternate method to determine the pK_a of histidine. Based on computational modeling, Miller and Corcelli predicted that deuteration of any of the histidine side-chain carbon atoms would provide a vibrational probe sensitive to the protonation state of the residue (14). Subsequent experiments by Hoffman et al. showed that C2-deuterated histidine (His-C2D) generates a unique, Raman-active C-D stretching vibration, the frequency of which is sensitive to both the protonation state and noncovalent interactions of the neighboring nitrogen atoms (Fig. 1; (15)). More recently, Pogostin et al. used this C2-D probe to determine the pK_a of histidine in the tripeptide AcNH-HVD-$CONH_2$ (which represents the C-terminal fragment of the peptide used in this study), validating their result using solution ^{1}H NMR spectroscopy (16).

Submitted August 19, 2020, and accepted for publication September 15, 2020.

*Correspondence: gabriel.braun@fulbrightmail.org

Editor: John Conboy.
https://doi.org/10.1016/j.bpj.2020.09.011

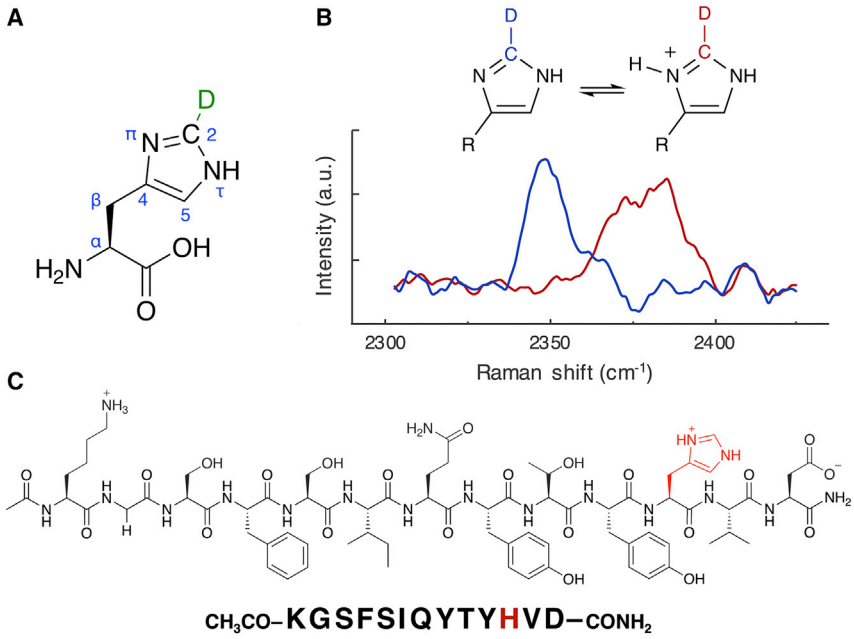

FIGURE 1 (*A*) His-C2D, with positions labeled according to current IUPAC guidelines (36). (*B*) The Raman-active, protonation-sensitive C2-D vibrational stretch is shown. Under acidic conditions (pH 2.0; *red curve*), histidine is doubly protonated, and the C2-D band is centered around 2385 cm^{-1}; under basic conditions (pH 10.5, *blue curve*), histidine is singly protonated, and the C2-D band is centered around 2350 cm^{-1}. (*C*) $SgI_{37–49}$, the hydrogel-forming peptide used in this study, is shown with the histidine residue highlighted in red.

Here, we report the determination of the pK_a of histidine in a hydrogel-forming peptide using this C2-D vibrational probe. The peptide $SgI_{37–49}$ (Fig. 1 *C*) self-assembles near neutral pH to form β-sheet hydrogel fibrils (Fig. S6), presumably driven by hydrophobic interactions that become possible after the neutralization of the peptide upon deprotonation of histidine (4). However, this hypothesis could not be easily verified by either solid-state or solution NMR because of the gel formed by $SgI_{37–49}$. To install the C2-D probe, we developed a method to incorporate His-C2D into $SgI_{37–49}$ during solid-phase peptide synthesis (SPPS). We then followed the shift of the C2-D vibrational stretch using Raman difference spectroscopy throughout a pH titration to determine the pK_a of the histidine residue, demonstrating the applicability of this probe to the study of self-assembling systems.

In previous studies, the C2-D probe was installed on the already-synthesized protein or peptide (15,16), using a well-established postsynthesis deuterium exchange reaction originally developed for NMR studies (17). However, this approach allows for little control over the locational specificity of the exchange, as exemplified by our attempts to perform this deuterium exchange on the tetrameric peptide AcNH-YHVD-$CONH_2$ (the four C-terminal residues of $SgI_{37–49}$), during which the unexpected addition of a second deuterium atom that could not be readily back exchanged was observed. Furthermore, this exchange protocol would be unsuitable for systems containing multiple exchangeable histidine residues because it would be extremely difficult to selectively deuterate a specific residue. We therefore sought a way to perform the deuterium exchange before peptide synthesis.

To perform SPPS with His-C2D, reactive sites on the amino acid must be protected to avoid unwanted reactions. Typically, a fluorenylmethyloxycarbonyl (Fmoc) group is added to the α-amino group to prevent addition of more than one residue to the growing peptide chain during each coupling step, and a trityl (Trt) group is added to the imidazole N^{τ} to both prevent unwanted side reactions and reduce the rate of histidine epimerization during peptide synthesis (18,19). However, we found that the elevated temperature deuterium exchange reaction could not be performed on Fmoc-His(Trt), which is widely commercially available, because loss of the Fmoc group occurred much more quickly than the deuterium exchange reaction. To obtain Fmoc-His(Trt)-C2D (**4**), we therefore performed the exchange reaction before the addition of the Fmoc and Trt groups (Fig. 2).

For the synthesis of **4**, it was necessary to use conditions that ensured full retention of the deuterium probe, which is labile under basic conditions at elevated temperature. An additional challenge was posed by the low solubility of both **3** and **4** because of the presence of the highly hydrophobic Trt and Fmoc groups. For the deuterium exchange, **1** was incubated in D_2O at pH 8.0 and 50°C before being lyophilized and redissolved in acidic, nondeuterated aqueous solution to back exchange readily exchangeable deuterium atoms. Trt protection was achieved by reacting **2** with Trt-Cl in the presence of dimethyldichlorosilane, using triethylamine as a base. Fmoc protection of **3** was achieved using Fmoc-Cl under Schotten-Baumann conditions with sodium carbonate as the base to give the desired product, **4**. Mass spectrometry was performed on the product after each step of the reaction to confirm the complete

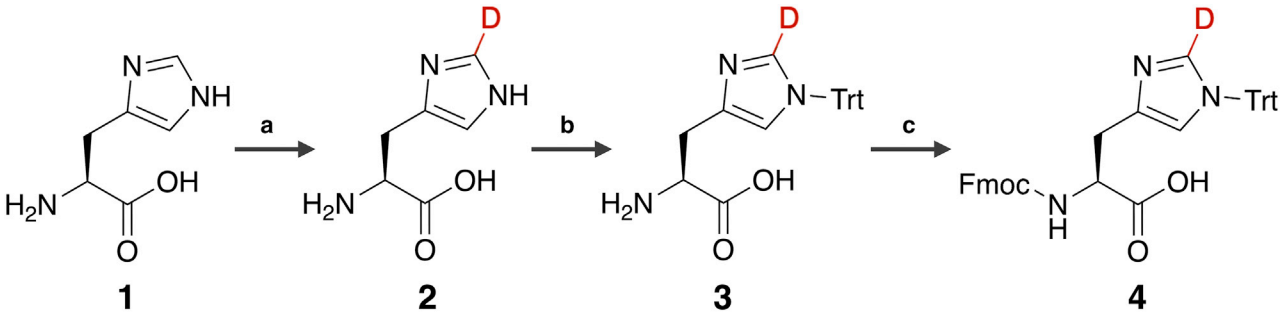

FIGURE 2 Synthesis of Fmoc- and Trt-protected, C2-deuterated histidine. Reaction conditions are as follows: (*a*) D_2O, NaOD (pH 8.0), 50°C, 72 h, then lyophilized; H_2O, HCl, then lyophilized, 100% yield; (*b*) dichloromethane, Me_2SiCl_2, reflux, 4 h; triethylamine, reflux, 15 min; Trt-Cl, triethylamine, 21°C, 12 h, 84% isolated yield; (*c*) tetrahydrofuran, 10% Na_2CO_3 (aq), Fmoc-Cl, 0–21°C, 1 h, 50% isolated yield. To see this figure in color, go online.

retention of the deuterium probe (Figs. S1 and S2). Compound **4** was then incorporated into $SgI_{37–49}$ using SPPS. Standard Fmoc-deprotection chemistry of 20% piperidine in dimethylformamide resulted in ~10% deuterium back exchange with each Fmoc-deprotection step. To counter this, a solution of 5% piperazine, 2% 1,8-diazabicyclo [5.4.0]undec-7-ene, and 1% formic acid in dimethylformamide was used instead (20). Using these conditions, the selectively C2-deuterated peptide ($SgI_{37–49}$-C2D) was successfully synthesized with full retention of the deuterium probe as confirmed by mass spectrometry (Fig. S3). This SPPS protocol should be generally useful for synthetic incorporation of His-C2D into any peptide.

To demonstrate the utility of the His-C2D probe in investigations of self-assembling systems, the frequency of the protonation-sensitive C2-D vibrational band was followed as a function of solution pH using Raman difference spectroscopy (Fig. 3). Aliquots of a solution of ~7 mM $SgI_{37–49}$-C2D in H_2O were pH adjusted to make a titration curve with steps of between 0.25 and 1 pH units. The C2-D stretching vibration displayed maxima around 2345 and 2380 cm^{-1} at high and low pH, respectively. These values are comparable to those reported by Hoffman et al. (15) and slightly lower than those reported in the study of the HVD tripeptide, for which a frequency shift of +10 cm^{-1} was noted in the low-frequency signal (16). Because of the relatively low intensity of the C2-D vibrational band, a pH 2.0 spectrum was subtracted from each subsequent sample to facilitate comparison of the spectral changes as a function of pH. This type of difference analysis is commonly used in vibrational spectroscopy of peptides and proteins to visualize changes between two states due to some sort of perturbation such as photolysis or ligand binding (16,21). In the difference spectra, the low-frequency vibration appears as a positive peak, corresponding to increasing concentration of the neutral histidine residue, whereas the high-frequency vibration appears as a negative peak, corresponding to decreasing concentration of the cationic residue. The intensity difference between the low- and high-frequency peaks was then plotted against sample pH (Fig. 3 *B*). A sigmoidal dose-response curve (Eq. S1), for which the midpoint corresponds to the pK_a-value, was fitted to the data. The pK_a of the histidine residue in $SgI_{37–49}$ was thus determined to be 5.66 ± 0.06. This pH titration was also performed using a home-built (rather than commercial) Raman spectrometer (Fig. S5); the pK_a-values determined from these two titrations agree within the error of the fitting parameters.

The pK_a-value determined here supports the hypothesis that the deprotonation of histidine leads to the pH-dependent self-assembly of $SgI_{37–49}$, which forms a weak gel above pH 5 and a robust gel above pH 6. The pK_a of histidine in $SgI_{37–49}$ determined in this experiment is slightly lower than the standard value for the second protonation of the solvated amino acid (pK_a = 6.0) (22). Interestingly, the pK_a of histidine in the full $SgI_{37–49}$ peptide is more than a full pK_a unit lower than that of the C-terminal tripeptide fragment of $SgI_{37–49}$ (pK_a = 6.82), which does not self-assemble (16). This increase in acidity is likely caused primarily by the hydrophobic environment in the fibril core of the aggregated neutral peptides, demonstrating the large impact that self-assembly can have on the pK_a of histidine. This is consistent with previous studies showing that self-assembly often leads to significantly shifted pK_a-values (by as much as 6.5 pK_a units), with the neutral species always favored (23–25), as is observed for $SgI_{37–49}$.

It is worth briefly considering the challenges that might be faced in applying this technique to other systems. One obvious limitation is that the length of the peptide into which His-C2D can be incorporated is constrained by the length limits of SPPS (~50 amino acids) (26). In principle, this can be readily overcome by using solution-phase segment condensation (26,27), native chemical ligation (28), or expressed protein ligation (28,29) to incorporate a His-C2D-containing peptide, synthesized using the methods described here, into longer sequences. A more pressing issue is the low intensity of the C2-D signal; despite working near the solubility limit of $SgI_{37–49}$, the weakness of the signal meant that it was necessary to use acquisition times of 12 h per Raman spectrum to obtain reliable data. For systems with lower solubility, it would likely be necessary to use techniques such as

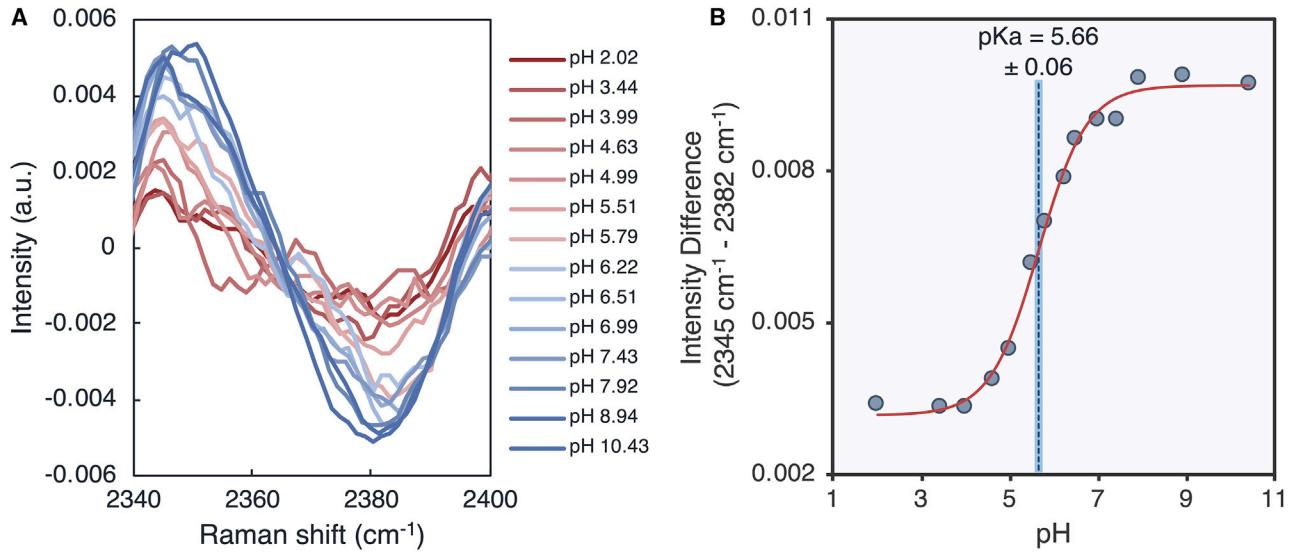

FIGURE 3 The pH titration of $SgI_{37–49}$-C2D. (*A*) Concentration-normalized Raman difference spectra are given, showing the C2-D stretching vibration. The positive band at 2350 cm^{-1} corresponds to the growth of the neutral form of the histidine imidazole; the negative band at 2380 cm^{-1} corresponds to the disappearance of the positively charged species. (*B*) The pH titration curve is shown. The red curve is a sigmoidal fit (Eq. S1), the midpoint of which corresponds to pK_a and is shown by the dashed line; the blue bar around the midpoint line shows the error in the fitting value.

surface-enhanced Raman spectroscopy (30), coherent anti-Stokes Raman scattering (31), or stimulated Raman scattering (32) to increase the Raman scattering cross section and clearly visualize the C2-D stretching vibration. This study demonstrates, however, that the His-C2D probe can be used without the aid of enhanced Raman techniques in systems with sufficiently high solubility.

In conclusion, we have shown here the applicability of the His-C2D vibrational probe to the investigation of heterogeneous soft materials through the example of a self-assembling peptide system. We synthesized a hydrogel-forming peptide, $SgI_{37–49}$, containing a selectively His-C2D residue. We then used Raman difference spectroscopy to track the protonation-sensitive shift of the distinctive C2-D-stretching vibration as a function of pH to determine the pK_a of this histidine residue, a task which would be extremely challenging using either solid-state or solution NMR spectroscopy. Both the synthetic and analytical methods used in this study can be readily applied to other systems. The protocol reported here for the synthesis of Fmoc-His(Trt)-C2D produces a probe-equipped amino acid that can be facilely incorporated into any target peptide through SPPS using relatively conventional conditions. This method also allows for the targeted C2-deuteration of a specific side chain in a peptide containing multiple histidine residues. Raman spectroscopy is a very flexible technique that is amenable to samples of arbitrary heterogeneity in a way that more conventional techniques are not. Although we have focused here on a self-assembling peptide, this probe could also be applied to investigations of histidine residues in nonself-assembling systems that are similarly difficult to study such as membrane-associated proteins and peptides. The method is not limited to pK_a determination because the C2-D stretching vibration has also been shown to report on noncovalent interactions involving the histidine imidazole such as H-bonding and metal coordination (15). We envision that, facilitated by the broadly applicable synthetic and analytical methods presented in this study, the His-C2D vibrational probe will prove to be a useful tool for investigating the physicochemical properties of histidine in many different peptide and protein systems.

SUPPORTING MATERIAL

Supporting Material can be found online at https://doi.org/10.1016/j.bpj.2020.09.011.

AUTHOR CONTRIBUTIONS

K.S.Å. and C.H.L. designed the research. B.H.P. and G.A.B. synthesized Fmoc-His(Trt)-C2D. $SgI_{37–49}$-C2D was synthesized and purified by G.A.B. and K.S.Å. Raman scattering experiments were performed by G.A.B. and M.P. Raman data were processed and analyzed by G.A.B. and C.H.L. The manuscript was written by G.A.B., K.S.Å., and C.H.L.

ACKNOWLEDGMENTS

The authors sincerely thank Jia Hu and Lou Charkoudian (Department of Chemistry, Haverford College) for performing and providing instrumentation for LCMS, respectively. The authors also gratefully acknowledge Per Persson (Centre for Environmental and Climate Research, Lund University) for providing instrumentation and technical expertise for Raman spectroscopy.

This work was supported by funding from Haverford College (K.S.Å.), the Fulbright U.S. Student Program (G.A.B.), and National Science Foundation grants CHE-1609291 (K.S.Å., from the MSN Program) and CHE-1800080 (C.H.L., from the CSDM-A Program).

SUPPORTING CITATIONS

References (33–35) appear in the Supporting Material.

REFERENCES

1. Kampmann, T., D. S. Mueller, …, B. Kobe. 2006. The role of histidine residues in low-pH-mediated viral membrane fusion. *Structure.* 14:1481–1487.
2. Malevanets, A., P. A. Chong, …, S. J. Wodak. 2017. Interplay of buried histidine protonation and protein stability in prion misfolding. *Sci. Rep.* 7:882.
3. Murtaugh, M. L., S. W. Fanning, …, J. R. Horn. 2011. A combinatorial histidine scanning library approach to engineer highly pH-dependent protein switches. *Protein Sci.* 20:1619–1631.
4. Frohm, B., J. E. DeNizio, …, S. Linse. 2015. A peptide from human semenogelin I self-assembles into a pH-responsive hydrogel. *Soft Matter.* 11:414–421.
5. Abedini, A., and D. P. Raleigh. 2005. The role of His-18 in amyloid formation by human islet amyloid polypeptide. *Biochemistry.* 44:16284–16291.
6. Lin, B. F., K. A. Megley, …, M. V. Tirrell. 2012. pH-responsive branched peptide amphiphile hydrogel designed for applications in regenerative medicine with potential as injectable tissue scaffolds. *J. Mater. Chem.* 22:19447–19454.
7. Shimba, N., Z. Serber, …, V. Dötsch. 2003. Quantitative identification of the protonation state of histidines in vitro and in vivo. *Biochemistry.* 42:9227–9234.
8. Hansen, A. L., and L. E. Kay. 2014. Measurement of histidine pKa values and tautomer populations in invisible protein states. *Proc. Natl. Acad. Sci. USA.* 111:E1705–E1712.
9. Schmidt, H. L. F., G. J. Shah, …, C. M. Rienstra. 2010. NMR determination of protein p$K_{(a)}$ values in the solid state. *J. Phys. Chem. Lett.* 1:1623–1628.
10. Li, S., and M. Hong. 2011. Protonation, tautomerization, and rotameric structure of histidine: a comprehensive study by magic-angle-spinning solid-state NMR. *J. Am. Chem. Soc.* 133:1534–1544.
11. Foster, M. P., C. A. McElroy, and C. D. Amero. 2007. Solution NMR of large molecules and assemblies. *Biochemistry.* 46:331–340.
12. Messinger, R. J., T. Vu Huynh, …, M. Deschamps. 2020. Magic-angle-spinning-induced local ordering in polymer electrolytes and its effects on solid-state diffusion and relaxation NMR measurements. *Magn. Reson. Chem* Published online August 23, 2020. https://doi.org/10.1002/mrc.5033.
13. El Hariri El Nokab, M., and P. C. A. van der Wel. 2020. Use of solid-state NMR spectroscopy for investigating polysaccharide-based hydrogels: a review. *Carbohydr. Polym.* 240:116276.
14. Miller, C. S., and S. A. Corcelli. 2010. Carbon-deuterium vibrational probes of the protonation state of histidine in the gas-phase and in aqueous solution. *J. Phys. Chem. B.* 114:8565–8573.
15. Hoffman, K. W., M. G. Romei, and C. H. Londergan. 2013. A new Raman spectroscopic probe of both the protonation state and noncovalent interactions of histidine residues. *J. Phys. Chem. A.* 117:5987–5996.
16. Pogostin, B. H., A. Malmendal, …, K. S. Åkerfeldt. 2019. pKa determination of a histidine residue in a short peptide using Raman spectroscopy. *Molecules.* 24:405.
17. Matsuo, H., M. Oe, …, K. Narita. 1972. A new approach to the determination of pKa's of histidine residues in proteins. *J. Biochem.* 72:1057–1060.
18. Sieber, P., and B. Riniker. 1987. Protection of histidine in peptide synthesis: a reassessment of the trityl group. *Tetrahedron Lett.* 28:6031–6034.
19. Hussein, W. M., M. Skwarczynski, and I. Tóth. 2020. Peptide Synthesis: Methods and Protocols. Humana, New York, NY.
20. Ralhan, K., V. G. KrishnaKumar, and S. Gupta. 2015. Piperazine and DBU: a safer alternative for rapid and efficient Fmoc deprotection in solid phase peptide synthesis. *RSC Adv.* 5:104417–104425.
21. Lorenz-Fonfria, V. A. 2020. Infrared difference spectroscopy of proteins: from bands to bonds. *Chem. Rev.* 120:3466–3576.
22. Rumble, J. R., D. R. Lide, and T. J. Bruno. 2019. CRC Handbook of Chemistry and Physics: A Ready-Reference Book of Chemical and Physical Data, Hundredth Edition. CRC Press, Boca Raton, FL.
23. Tang, C., A. M. Smith, …, A. Saiani. 2009. Fmoc-diphenylalanine self-assembly mechanism induces apparent pK_a shifts. *Langmuir.* 25:9447–9453.
24. Mondal, J., X. Zhu, …, A. Yethiraj. 2012. Sequence-dependent pK_a shift induced by molecular self-assembly: insights from computer simulation. *J. Phys. Chem. B.* 116:491–495.
25. Tena-Solsona, M., J. Nanda, …, B. Escuder. 2016. Emergent catalytic behavior of self-assembled low molecular weight peptide-based aggregates and hydrogels. *Chemistry.* 22:6687–6694.
26. Raibaut, L., O. El Mahdi, and O. Melnyk. 2014. Solid phase protein chemical synthesis. *In* Protein Ligation and Total Synthesis II. L. Liu, ed. Springer International Publishing, pp. 103–154.
27. Kimmerlin, T., and D. Seebach. 2005. '100 years of peptide synthesis': ligation methods for peptide and protein synthesis with applications to beta-peptide assemblies. *J. Pept. Res.* 65:229–260.
28. Conibear, A. C., E. E. Watson, …, C. F. W. Becker. 2018. Native chemical ligation in protein synthesis and semi-synthesis. *Chem. Soc. Rev.* 47:9046–9068.
29. Berrade, L., and J. A. Camarero. 2009. Expressed protein ligation: a resourceful tool to study protein structure and function. *Cell. Mol. Life Sci.* 66:3909–3922.
30. Fan, M., G. F. S. Andrade, and A. G. Brolo. 2011. A review on the fabrication of substrates for surface enhanced Raman spectroscopy and their applications in analytical chemistry. *Anal. Chim. Acta.* 693:7–25.
31. Cheng, J.-X. 2007. Coherent anti-stokes Raman scattering microscopy. *Appl. Spectrosc.* 61:197–208.
32. Tipping, W. J., M. Lee, …, A. N. Hulme. 2016. Stimulated Raman scattering microscopy: an emerging tool for drug discovery. *Chem. Soc. Rev.* 45:2075–2089.
33. Zandomeneghi, G., M. R. H. Krebs, …, M. Fändrich. 2004. FTIR reveals structural differences between native beta-sheet proteins and amyloid fibrils. *Protein Sci.* 13:3314–3321.
34. Lomont, J. P., J. S. Ostrander, …, M. T. Zanni. 2017. Not all β-sheets are the same: amyloid infrared spectra, transition dipole strengths, and couplings investigated by 2D IR spectroscopy. *J. Phys. Chem. B.* 121:8935–8945.
35. Ghosh, A., J. S. Ostrander, and M. T. Zanni. 2017. Watching proteins wiggle: mapping structures with two-dimensional infrared spectroscopy. *Chem. Rev.* 117:10726–10759.
36. IUPAC. 2009. IUPAC Compendium of Chemical Terminology: the Gold Book, Version 2.1.0. IUPAC, Research Triagle Park, NC.